

Preserving Overall Performance of Air Conditioners by Incorporation of Wind-permeable Floor in Buildings

Karl An^{1*}, Ross Y M Wong⁴, Kelvin K F Sin², Jimmy C H Fung^{1,3}, Zhigang Li²

¹Division of Environment, The Hong Kong University of Science and Technology, Clear Water Bay, Hong Kong

²Department of Mechanical and Aerospace Engineering, The Hong Kong University of Science and Technology, Clear Water Bay, Hong Kong

³Department of Mathematics, The Hong Kong University of Science and Technology, Clear Water Bay, Hong Kong

⁴AECOM Asia Co. Ltd., Shatin, Hong Kong

*Corresponding email: karlanlok@ust.hk

1. Introduction

Hong Kong is one of the most extensively urbanized areas in the world with high population density. Extensive mechanical ventilations are essential to provide space cooling and thermal comfort for occupants. Unitary air conditioners are ubiquitously installed at the re-entrants of buildings, operating continuously and concurrently, generating and releasing a vast amount of anthropogenic heat. These heat emissions have a large impact upon the local microclimate of a city. One of the best known effects is the urban heat island (UHI) phenomenon (Lo et al. 1997 [1]).

This study focuses on the residual heat ejected by outdoor condensing units that is accumulated within semi-enclosed re-entrants of buildings. The energy conversion efficiency of air conditioners would be degraded due to high working temperature. Bojic et al. (2001) [2] demonstrated by computational fluid dynamic simulations that temperature difference between rooftop and ground level of a typical 30 storey building could reach 7°C, while Bruelisauer et al. (2014) [3] showed by field measurement a temperature difference of at least 10°C over a 24 storey building. Moreover, Chow et al. (2000) [4] reported that overall percentage drop in coefficient of performance (COP) of air conditioners could reach a maximum of 26% under no-wind condition. In addition, Chow et al. (2002) [5] attempted to relocate the air conditioners for mitigation. Wind advection and thermal buoyancy are two important factors which mainly drive the motion of hot air stream, imposing vertical temperature gradients at the re-entrants of buildings. Architectural designs such as incorporation of an open wind-permeable floor may be helpful to alleviate thermal stack effect and conserve energy for space cooling. Elevated temperature in the re-entrants may degrade energy conservation efficiency of air conditioners. To alleviate thermal stack effect and conserve energy for space cooling, effectiveness of incorporating a wind permeable floor is investigated by Computational Fluid Dynamics (CFD) simulations in this study. Steady RANS simulations under various wind intensities and atmospheric stability conditions are carried out on a typical single residential block with and without a wind-permeable floor. Temperature profiles are plotted at various re-entrant locations. Group performances of the air conditioners, indicated by Condenser Group Performance Index (CGPI) are also calculated for the simulation cases. Over 10% enhancement of CGPI is achieved by the incorporation of wind permeable floor.

2. Theoretical Background

Resulting from surface layer flow over terrain with heat exchange, thermal stability can be characterized by Monin-Obukhov (M-O) length $L = u_*^2 T_0 / \kappa g \theta_*$, where $\theta_* = -q_0 / \rho c_p u_*$ is the scaling temperature, $c_p = 1006.43 \text{ J/kg-K}$ is the specific heat capacity at constant pressure for air, u_* is the frictional velocity, T_0 and q_0 are the surface temperature and the surface heat flux respectively. Atmospheric boundary layer (ABL) is neutral when $L = 0$. It is stable when $L > 0$, while it is unstable for $L < 0$. The gradients of wind velocity u and potential temperature θ can be expressed as universal functions of $\xi = z/L$ and written as $(\kappa z / u_*) \partial u / \partial z = \varphi_m(\xi)$ and $(\kappa z / \theta_*) \partial \theta / \partial z = \varphi_h(\xi)$

ICUC9 – 9th International Conference on Urban Climate jointly with 12th Symposium on the Urban Environment respectively, where $\varphi_m(\xi) = \varphi_h(\xi) = 1 + 5\xi$ for $L > 0$; and $\varphi_m(\xi) = (1 - 16\xi)^{-1/4}$ and $\varphi_h(\xi) = (1 - 16\xi)^{-1/2}$ for $L < 0$, which are the stability functions (Dyer (1974) [6]). Upon integration, u and θ can be expressed in terms of z explicitly by:

$$u(z) = \frac{u_*}{\kappa} \left[\ln \left(\frac{z}{z_0} \right) - \Psi_m \left(\frac{z}{L} \right) \right] \quad (1)$$

and

$$\theta(z) = \theta_0 + \frac{\theta_*}{\kappa} \left[\ln \left(\frac{z}{z_0} \right) - \Psi_h \left(\frac{z}{L} \right) \right] \quad (2)$$

where $\Psi_{m(h)}(\xi) = \left(\int_0^\xi \varphi_{m(h)}(\xi') d\xi' \right) / \xi$, z_0 is the aerodynamic roughness length and θ_0 is the potential temperature at ground. θ can be related to absolute temperature T by $\partial\theta/\partial z = \partial T/\partial z + g/c_p$. Eqn. (1) and (2) represent the equilibrium velocity and temperature profiles of ABL flow over flat terrain under various thermal stratifications. On the other hand, ABL flow and associated heat transfer phenomena can be described by RANS equations with turbulence modeling equations. As proposed by Alinot and Masson (2005) [7] and validated by Pieterse and Harm (2013) [8], non-zero source terms $S_T = -g(\partial\mu_t/\partial z)/\sigma_T$, $S_k = \beta g\mu_t(\partial T/\partial z - g/c_p)/\sigma_T$ and $S_\varepsilon = (1 - C_{3\varepsilon})C_{1\varepsilon}S_k \varepsilon/k$, where $\mu_t = \rho C_\mu k^2/\varepsilon$ is the turbulent viscosity, $\sigma_T = 0.85$, $C_\mu = 0.09$ and $C_{1\varepsilon} = 1.44$ are the constants for standard $k - \varepsilon$ turbulence model and $\beta = 0.00343/K$ is the thermal expansion coefficient, should be added to energy, turbulent kinetic energy and turbulent dissipation rate equations respectively to account for buoyant production of turbulence while preserving stream wise homogeneous velocity and temperature profiles.

3. Homogeneity of Stream wise Velocity and Temperature Profiles in CFD Simulations

CFD simulation package, ANSYS FLUENT 14.5, is used for the simulations. A three dimensional empty rectangular domain with 2000m x 1000m x 600m (L x W x H) in size is created to investigate the self-maintenance of the velocity and temperature profiles in the stream wise direction. Velocity inlet boundary condition is applied at the inflow and the top boundary with flow, turbulence and thermal quantities. Standard wall function is applied at the bottom surface. As suggested by Blocken et al. (2007) [9], bottom surface roughness height k_s is set to a value of $20z_0$. Symmetry boundary conditions are applied at the lateral sides. Zero gradient boundary condition is applied at the outflow face. An approximate of 1.5 million structural cells are created with the first cell height of 0.5m. A grid expansion ratio of at most 1.2 is maintained in both horizontal and vertical directions as recommended by COST C14 (Franke et al., 2004 [10]).

Table 1 tabulates the various parameters for the inflow profiles under different simulated cases. Inflow velocity and temperature profiles defined by Eqns. (1) and (2) with turbulence kinetic energy and dissipation profiles defined by $k(z) = (u_*^2/\sqrt{C_\mu})\sqrt{\varphi_\varepsilon(z)/\varphi_m(z)}$ and $\varepsilon(z) = u_*^3\varphi_\varepsilon(z)/\kappa z$ respectively, where $\varphi_\varepsilon(z) = 1 - z/L$ for $L < 0$ and $\varphi_\varepsilon(z) = \varphi_m(z/L) - z/L$ for $L > 0$ (Pieterse and Harm (2013) [8]) are imposed at the inflow face. Second Order Upwind Schemes are used for the advection terms of governing equations. Least square cell based gradient scheme is applied for the diffusion term and PRESTO! Scheme for the pressure term. Pressure-velocity coupling is handled by SIMPLE algorithm. The discretized governing equations are solved iteratively until all the scaled residuals are drop below 1×10^{-6} (Casey and Wintergeste, 2000 [11]). **Figure 1** depicts the velocity and temperature profiles at various downstream distance at the center line away from the inflow face under neutral, stable and unstable atmospheric conditions. The results have shown that after addition of various source terms with appropriate inflow conditions, homogeneity of velocity and temperature profiles can be achieved.

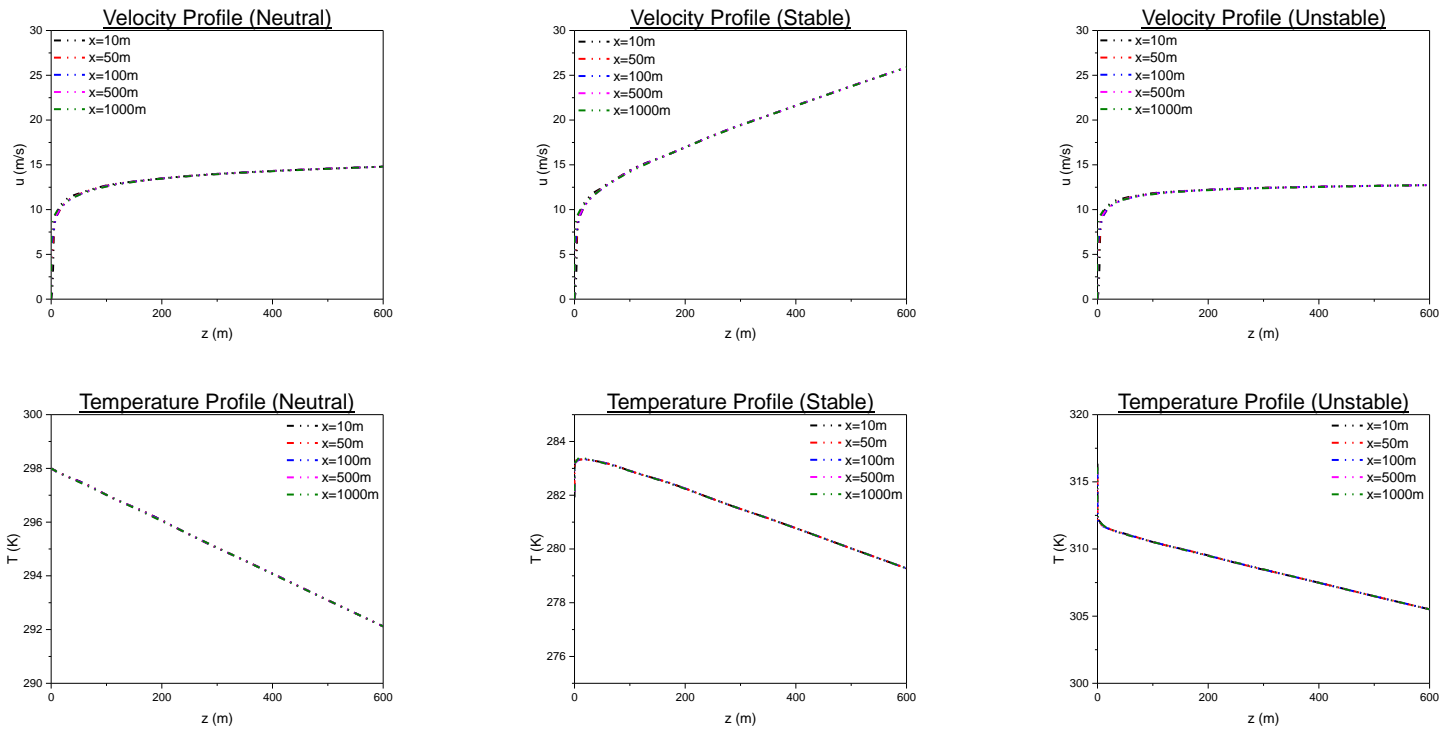


Figure 1 Velocity and temperature profiles at various distance from inlet under neutral, stable and unstable thermal stratification

	Stability Class	z_0 (m)	u_* (m/s)	q_0 (W/m ²)	θ_0 (K)	L (m)
1	Neutral	0.002	0.4815	0	298	∞
2	Stable	0.002	0.473	-30	283	306.0
3	Unstable	0.002	0.5085	100	313	-126.1

Table 1 Various parameters of the inflow profiles for the empty domain case

4. Geometry and CFD Parameter Settings for the Study Cases

Air flow and heat transfer around a typical 30 storey (3m per floor) cross shaped residential building in Hong Kong is investigated in this study. Two buildings, one with a 5m wind-permeable floor located between 15th and 16th floor and one without the wind permeable floor are studied. **Figure 2** shows the layout and dimensions of the subjected buildings. Radiated from the building core, residential units at the same wing are separated by a recessed area. Air conditioners are placed at the vertically extended semi-enclosed building re-entrants. At each floor, 4 air conditioners are placed at the same re-entrants. Each air conditioner is modeled by a volumetric heat source, generating 2500W of heat.

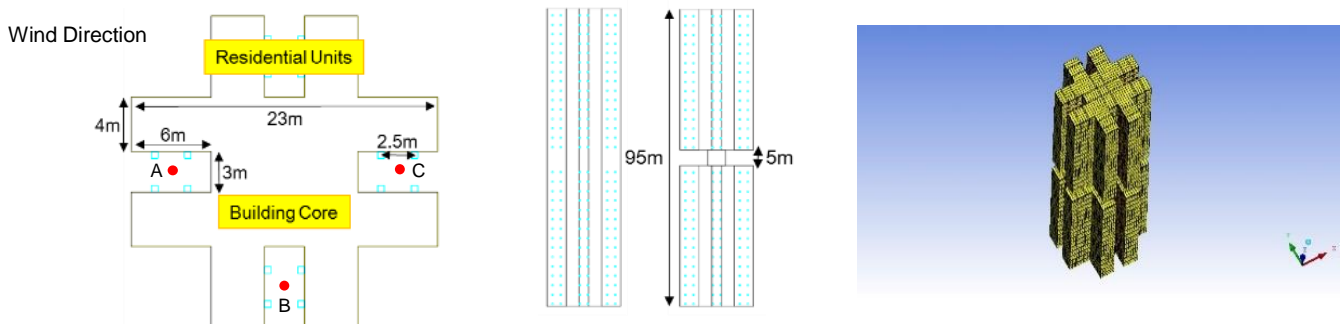


Figure 2 Geometry Layout and mesh of the simulated building

The full scale building is placed within the computational domain of approximately 3 million structural grids with a distance of 5H (where H=95m is the building height) from the upstream, lateral and top boundaries and 15H away from the downstream boundary as recommended by Franke, 2011 [12] and Tominaga et al., 2008 [13] to minimize the influence of the boundaries to the interested region. The building wall is set as no slip boundary condition while other parameters settings (apart from the inflow profiles) are consistent with the validation cases. Each of the 9 cases (9 cases for the building with wind permeable floor and 9 cases for the building without one) are divided into 3 categories with inflow profiles representing neutral, stable and unstable thermal stratifications respectively. Furthermore, while maintaining the temperature difference ΔT between ground and rooftop are kept consistent under same atmospheric stability, influence of wind magnitudes on the effectiveness of the permeable floor are also studied by imposing inflow velocity profiles with varying wind speeds u_{10} at 10m above ground (i.e. $u_{10}=2.5\text{m/s}$, 5m/s and 10m/s). The parameters of the inflow velocity and temperature profiles for different cases are listed in **Table 2**.

	Stability Class	z_0 (m)	u_* (m/s)	u_{10} (m/s)	q_0 (W/m ²)	θ_0 (K)	ΔT (K)	L (m)
1	Neutral	0.002	0.1205	2.5	0	303	0.98	∞
2	Neutral	0.002	0.2405	5	0	303	0.98	∞
3	Neutral	0.002	0.4815	10	0	303	0.98	∞
4	Stable	0.002	0.102	2.5	-3.04	303	-0.57	32.42
5	Stable	0.002	0.227	5	-11.14	303	-0.57	97.52
6	Stable	0.002	0.473	10	-30	303	-0.57	327.62
7	Unstable	0.002	0.1545	2.5	40.5	303	4.52	-8.46
8	Unstable	0.002	0.2745	5	61.4	303	4.52	-31.29
9	Unstable	0.002	0.5085	10	100	303	4.52	-122.12

Table 2 Various parameters of the inflow profiles in different CFD simulation cases

5. Results and Discussion

Figure 3 plots the temperature profiles at three locations A, B and C of re-entrants of the building at the windward, sideward and leeward sides respectively. At location A, similar behavior of the temperature profiles are observed for both cases with/without permeable floor under different atmospheric stability conditions. It is also interesting to notice that different wind speed magnitude would have minor influence on the magnitude and shape of temperature profiles at the windward side. At location B (sideward), there is a temperature drop of approximately 5°C with the implementation of the permeable floor. In addition, a drop of temperature from approximately 314K to 305K is observed under the neutral atmosphere with low inflow wind speed. Comparing to the cases without the merit design, the temperature maintains an increment trend which is an evidence of the continuous accumulation of the heat emitted from the air conditioners. However, under the stable and unstable atmospheric conditions, although temperature decline is also observed at the permeable floor location, it is not as significant when compared to the cases under the neutral atmosphere with relatively low wind speed. Furthermore, difference in magnitude in wind speed has minor effect on the temperature profiles near the permeable floor location under the stable and unstable atmospheric environment which is in contrast to the situation under the neutral atmosphere. At location C, the temperature drop at the open permeable floor for the cases under stable atmospheric conditions are not as obvious those cases under the neutral and unstable atmosphere. Under the neutral and unstable atmosphere, a minor drop

ICUC9 – 9th International Conference on Urban Climate jointly with 12th Symposium on the Urban Environment of 0.5 °C is observed for the cases with mid/high inflow wind magnitude while an observable drop of approximately 1 °C to 2 °C is revealed for the low wind cases. Despite the fact that there is decline in temperature at the re-entrant of the leeward side, the drop is not as sharp when compared to the sideward re-entrant at location B.

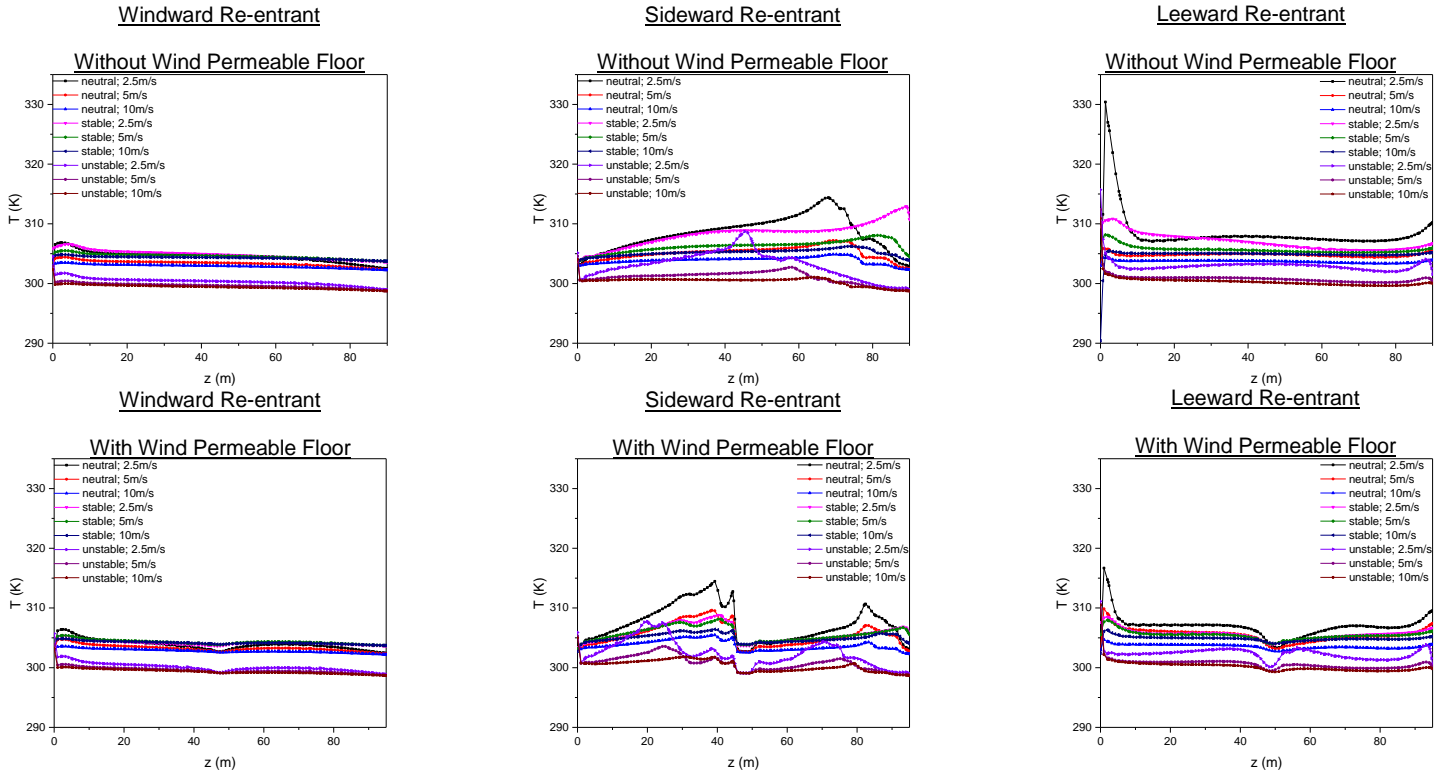


Figure 3 Temperature profiles at Locations A, B and C for different simulation cases

Cooling efficiency of an individual air conditioner can be quantified by coefficient of performance (COP), which is the ratio of cooling capacity to input electricity. COP depends on indoor temperature T_r and on-coil temperature of air conditioner T_{coil} . At specified T_r , COP drops linearly with T_{coil} by

$$COP_{T_r}(T_{coil}) = a - b(T_{coil} - 273) \quad (3)$$

where $a = 5.15$ and $b = 0.0738$ at $T_r = 298K$ obtained by linear regression of manufacturing data of commercially available split type air conditioners (Chow et al. (2000)[4]). COP acquires a value 2.94 at outdoor temperature T_{ref} of 303K. For n air conditioners working together, Condenser Group Performance Indicator (CGPI) is defined by:

$$CGPI_{T_r}(T_{ref}) = \frac{100}{n} \sum_{i=1}^n \left\{ 1 - \left[\frac{COP_{T_r}(T_{coil})}{COP_{T_r}(T_{ref})} \right]_i \right\} \quad (4)$$

CGPI is evaluated at $T_r = 298K$, $T_{ref} = T_0 = 303K$ and T_{coil} extracted from the simulated temperature at geometric center of air conditioners. **Figure 4** shows the CGPI value before and after implementation of wind-permeable floor in a building. Improvement of at least 10% is signified under neutral and stable stratifications, which is in line with the temperature drop in re-entrants observed near the wind permeable floor. Thus, it is shown that incorporation of wind-permeable floor in buildings is affirmative to conserve air-conditioning energy consumption of air conditioners under group operation.

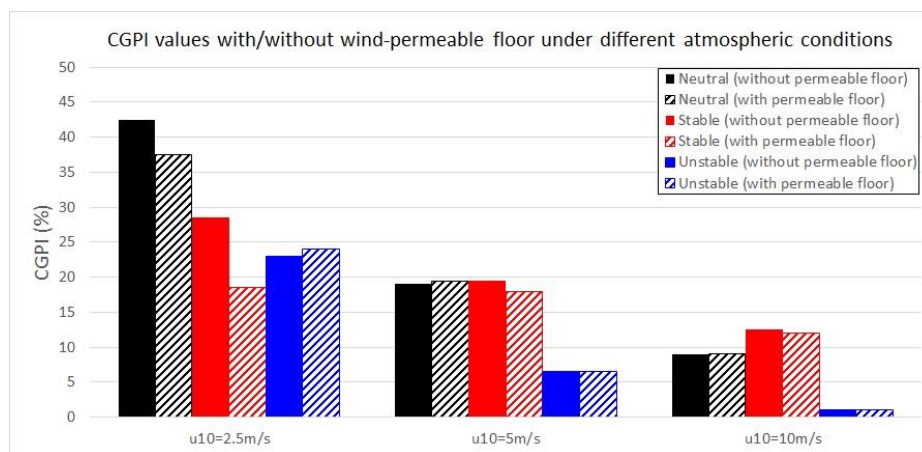


Figure 4 CGPI values before and after implementation of wind-permeable floor under different atmospheric conditions

6. Conclusion

The CFD simulation results show that after the implementation of an open permeable floor in residential blocks, elevated air passing through the floor is cooled by natural means. The residents above the permeable floor are expected to benefit from better thermal comfort than those below it. Performance of air conditioners are retained as a result of lower operating temperature, especially for those installed above the wind-permeable floor. The cooling effect by permeable floor is shown to be relatively significant for the neutral low wind magnitude cases compared to other atmospheric stability cases with higher wind speed. Developers/Architects may make reference to the results in the study as the incorporation of permeable floors is effective in reducing the thermal stack effect. To conclude, permeable floors can be considered as one of the potential mitigation measures, if necessary, in design/architectural studies in order to reduce the negative impacts on human thermal comfort to a minimal level.

References

- Lo C P, Quattrochi D A, Luvall J C (1997) Application of high resolution thermal infrared remote sensing and GIS to assess the urban heat island effect. *International Journal of Remote Sensing*, 18, 287–304
- Bojic M, Lee M, Yik F, (2001) Flow and temperature outside a high-rise residential building due to heat rejection by its air-conditioners, *Energy and Buildings* 33, 737 – 751
- Bruelisauer M, Meggers F, Saber E, Li C, Leibundgut H, (2014) Stuck in a stack – Temperature measurements of the microclimate around split type condensing units in a high rise building in Singapore, *Energy and Buildings* 71, 28 – 37
- Chow T T, Lin Z, Wang Q W, (2000) Effect of building re-entrant shape on performance of air-cooled condensing units, *Energy and Buildings* 32, 143 – 152
- Chow T T, Lin Z, Liu J P, (2002) Effect of condensing unit layout at building re-entrant on split-type air conditioner performance, *Energy and Buildings* 34, 237 – 244
- Dyer A J, (1974) A review of flux-profile relationship, *Boundary Layer Meteorology* 7, 363 – 372
- Alinot C, Masson C, (2005) k-e model for the atmospheric boundary layer under various thermal stratifications, *Journal of Solar Energy Engineering* 127, 438-443
- Pieterse J E, Harms T M, (2013) CFD investigation of the atmospheric boundary layer under different thermal stability conditions, *Journal of Wind Engineering and Industrial Aerodynamics* 121, 82-97
- Blocken B, Stathopoulos T, Carmeliet, J (2007) CFD simulation of the atmospheric boundary layer: wall function problems. *Atmos. Environ.* 41, 238–252
- Franke J, Hirsch C, Jensen A G, Krüs H W, Schwartzman M, Westbury P S, Miles S D, Wisse J A, Wright N G (2004). Recommendations on the use of CFD in wind engineering, In J.P.A.J. van Beek (Ed.), *Proc. Int. Conf. on Urban Wind Engineering and Building Aerodynamics: COST C14 – Impact of Wind and Storm on City life and Built Environment*, Rhode-Saint-Genèse
- Casey M, Wintergerste T (2000) *Quality and Trust in Industrial CFD: Best Practice Guidelines*. ERCOTFAC
- Franke J, Hellsten A, Schluenzen K, Carissimo B (2011) The COST 732 best practice guideline for CFD simulation of flows in the urban environment: a summary. *International Journal of Environment and Pollution*, vol. 44, p. 419 – 427
- Tominaga Y, Mochida A, Yoshie R, Kataoka H, Nozu T, Yoshikawa M (2008) AIJ guidelines for practical applications of CFD to pedestrian wind environment around buildings. *Journal of Wind Engineering and Industrial Aerodynamics*. 96:1749-61